ChemComm
Chemical Communications

Accepted Manuscript

This article can be cited before page numbers have been issued, to do this please use: S. Joshi, G. Mahadevan, S. Verma and S. Valiyaveettil, *Chem. Commun.*, 2020, DOI: 10.1039/D0CC04909C.

This is an Accepted Manuscript, which has been through the Royal Society of Chemistry peer review process and has been accepted for publication.

Accepted Manuscripts are published online shortly after acceptance, before technical editing, formatting and proof reading. Using this free service, authors can make their results available to the community, in citable form, before we publish the edited article. We will replace this Accepted Manuscript with the edited and formatted Advance Article as soon as it is available.

You can find more information about Accepted Manuscripts in the Information for Authors.

Please note that technical editing may introduce minor changes to the text and/or graphics, which may alter content. The journal's standard Terms & Conditions and the Ethical guidelines still apply. In no event shall the Royal Society of Chemistry be held responsible for any errors or omissions in this Accepted Manuscript or any consequences arising from the use of any information it contains.

ROYAL SOCIETY OF CHEMISTRY

rsc.li/chemcomm

View Article Online
DOI: 10.1039/D0CC04909C

COMMUNICATION

Bioinspired Adenine-Dopamine Immobilized Polymer Hydrogel Adhesives for Tissue Engineering

Received 00th January 20xx,
Accepted 00th January 20xx

DOI: 10.1039/x0xx00000x

Saurabh Joshi,[a,b] Gomathi Mahadevan,[a] Sandeep Verma,*[b] Suresh Valiyaveettil*[a]

Nontoxic adhesive hydrogels are of great importance in tissue engineering. Herein, we report a simple synthesis of a few biocompatible hydrogels from adenine and dopamine immobilized polyacrylic acid (PAA) and alginic acid (Alg) polymers. The adenine - dopamine adduct incorporated hydrogels showed enhanced adhesiveness, transparency, biocompatibility and induced cell proliferation in 2D and 3D-cell culture models within 24 hr. Moreover, blending the modified PAA and Alg polymers (P2P4) further increased the stability and bioactivity of the hydrogel. Such biogels can be developed as smart materials for biomedical applications.

Hydrogels are interesting materials owing to their functional characteristics similar to biological tissues with a range of physical and chemical properties.[1] Adhesive hydrogels have been used in different applications such as regenerative medicines,[2] wound healing,[3] and tissue engineering.[4, 5]Hydrogels with 3D networks can mimic the structure and functions of tissue microenvironment for monitoring cellular behaviour and properties.[6,7] Cells showed different growth patterns in two dimensional (2D) and three dimensional (3D) cell culture models.[8] Despite the fact that 3D cell culture is closer to an *in vivo* model, it is not widely used as a cellular model owing to many practical difficulties, which include poor reproducibility and low performances.[9]

Natural biopolymers are considered as good candidates for preparing hydrogels for biomedical applications.[10, 11] Chemical modifications are necessary to introduce appropriate functional groups to improve the interactions between the gel and cell surface. Nucleobases present in cellular DNA play an important role towards controlling overall health and functions of living tissues.[12] Nucleobases and their derivatives form functional supramolecular structures through intermolecular hydrogen bonds.[13] Even though catechol groups show active roles in many biological systems, the chemistry of catechol derivatives is not well explored in the design of new materials.[14] The nucleobases, especially adenine and dopamine incorporated polymeric hydrogels are not yet tested for cell adhesion or cell signaling.[15]

Polyacrylic acid (PAA) and alginic acid (Alg) based gels show good swelling behaviour, pH sensitivity, and accessible for further chemical modifications to obtain adhesive materials.[16-18] Unlike reported hydrogels from adenine or dopamine functionalized polymers, here we prepare an adenine-dopamine adduct and immobilize on the PAA or Alg polymer backbone (SI, Scheme S1A). This strategy allowed us to control the concentration & distribution of the bioactive molecules and to include the adenine-dopamine adduct inside a three-dimensional gel. The properties of such hydrogels are compared with the gels prepared from adenine functionalized PAA or Alg polymer. Our design strategy, synthetic scheme and the characterization details of the polymers are given in the supporting information (Figure S1-S9).

Functionalized adenine (**3**) and adenine-dopamine adduct (**6**) were synthesized using a reported procedure (SI, Scheme 1B). Polymers, **P1–P4** were synthesized by functionalizing PAA or Alg polymer with **3** and **6** using the literature procedure (Figure 1, Scheme S1 C, D).[19, 20] All final polymers, **P1–P4** are characterized using NMR and UV-Vis spectroscopy where the appearance of new peaks in the aromatic region corresponds to the incorporation of adenine and dopamine moieties on the polymer backbone (Figure S10-S11).

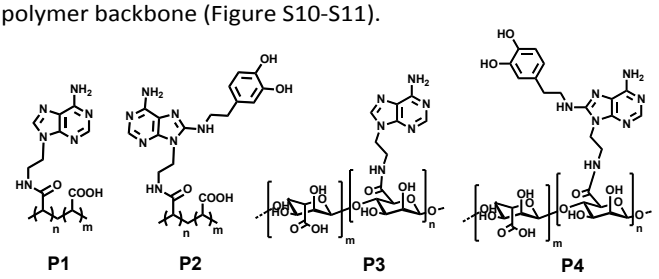

Figure 1. Molecular structures of synthesized polymers **P1-P4**.

The degree of conjugation is calculated using NMR spectra of the polymers **(P1-P4)**[17]by taking the ratio of integration of adenine's or dopamine hydrogen peaks in the aromatic region to the C-H peaks of the polymer backbone. The data show a

[a] *Department of Chemistry, National University of Singapore, 3 Science Drive 3, Singapore 117543.*
[b] *Department of Chemistry, Indian Institute of Technology Kanpur, Kanpur, Uttar Pradesh 208016, India.*
Electronic Supplementary Information (ESI) available:See DOI: 10.1039/x0xx00000x

low degree of functionalization (0.1 %) of adenine or adenine–dopamine adducts on the polymer backbone for **P1&P2**. The functionalized polymers were then cross-linked to form a gel, as confirmed by tube upside-down test (Figure S12&S13).[21] The gels from **P1**&**P2** are transparent and the observed light yellow colour of the **P2** gel is due to dopamine oxidation (Figure 2A). The freeze-dried hydrogels showed porous morphologies in SEM micrographs (Figure S14).

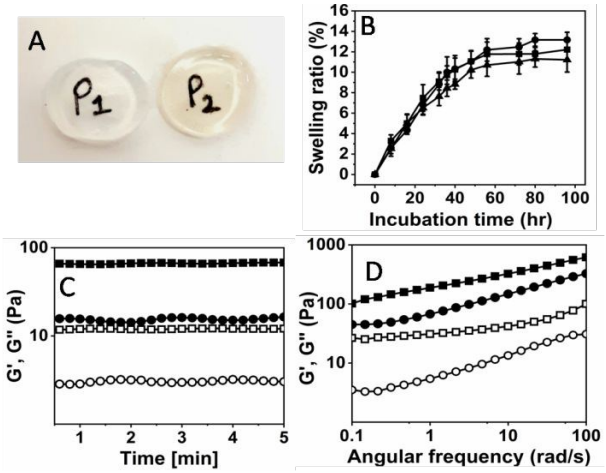

Figure 2. Transparent hydrogels (A) prepared from **P1** and **P2.** Swelling ratio curve (B) for **P1** (—■—), **P2** (—●—) and pure PAA (—▲—). Rheological properties – change in storage modulus G' for **P1** (—□—) and **P2** (—■—) and change in loss modulus G" for **P1** (—○—) and **P2** (—●—) with respect to time (C) and frequency (D)

Swelling ratio of hydrogels (5% w/v) was investigated by incubating them in phosphate buffered saline (PBS) solution for 96 hr (Figure 2B). Swelling ratio curves indicate that **P1** and **P2** hydrogels swelled with a same rate initially, but **P2** showed a slightly higher swelling rate after 24 hr, while PAA showed a relatively lower swelling rate (Figure 2B). The presence of polar groups such as adenine and dopamine plays a significant role towards interacting and stabilizing water molecules as swelling ratio decreased in the order of **P2**>**P1**>**PAA**.

The viscoelastic nature of hydrogels (5% w/v) was studied to understand the role of dynamic stiffening of hydrogels under different environments.[22] The changes in G' (storage modulus) and G" (loss modulus) at a fixed frequency of 1 Hz for 5 min shows a higher value of G' throughout the time period than G" showing an elastic nature of hydrogels from both **P1** and **P2** (Figure 2C). Moreover, the same trend was observed for angular frequency range from 0.1-100 rad/s (Figure 2D). Both gels showed consistent stability under low and high strain (Figure S15). The elastic modulus at 1 rad/s for **P2** (188 Pa) was higher than **P1** (31 Pa), which can be attributed to the increase in hydrophobic and hydrophilic interactions among the polymer chains due to the incorporation of adenine-dopamine adduct on the polymer backbone (Figure S12). The results also suggest the soft nature of the gels, which mimic similar properties of the extracellular matrix (ECM).

Nucleobase incorporated hydrogels are known for strong interactions with diverse substrates under various conditions.[23, 24] The adhesive behaviour of **P2** gel with adenine-dopamine adduct as anchors to the surface was examined in detail using various substrates. The gel was placed on top of various substrates for 5s and then it was lifted up for checking the adhesion (Figure S16). It showed excellent adhesivity to all hard and soft substrates including biological samples such as human and pork skin (Figure S16). Also, the gel did not leave any residue when peeled off from the surfaces implying good cohesive interactions (Figure S17). The pork skin was wet, moist and greasy, especially from the inside, but the **P2** hydrogel stuck to pork skin surface strongly suggesting the adhesion ability to the wet surfaces. To validate the findings, quantification of the adhesive strength of **P1&P2** gels with different substrates such as glass, aluminium and bio-tissues like pork skin were done using texture analysis method (Figure S18, Video S1).[25] Adhesiveness was obtained with respect to work done or force required to detach the probe from the samples and expressed as a negative value (Figure 3A). Adhesive strength decreases in the order of **P2**>**P1**>**PAA**, reflecting the strong interaction between the functional groups on the polymer backbone and different substrates (Figure 3B). **P2** has adenine-dopamine adduct on the backbone to impart adhesive interactions with substrates while **P1** only has adenine groups. The adhesive strength of the gels on glass surface was low for PAA (-2.2±0.6 g.s), followed by **P1** (-11±2 g.s) and **P2** with highest value (-28.7±6.5 g.s) (Figure 3B). Similar trend was also observed in the case of aluminium and pork skin substrates. Polymer **P2** showed highest adhesive strength of -196±15 g.s followed by **P1** (-98.33±10.04 g.s) on pork skin (Figure 3B). The same trend was observed for the hardness and cohesive strength of **P1** and **P2** (Figure 3C&D).

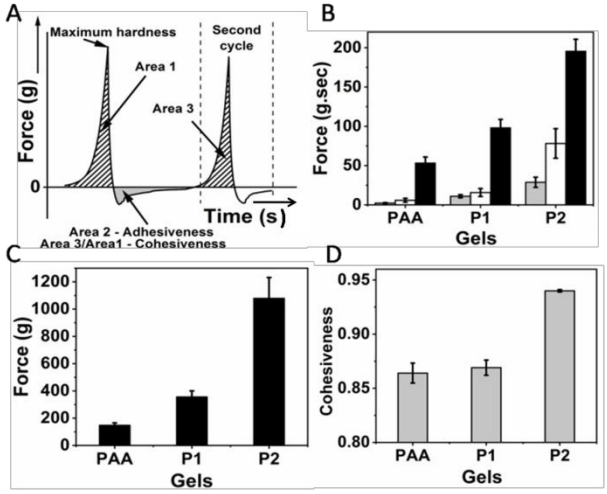

Figure 3. Schematic representation of the graph obtained from the texture analysis (A), adhesive strength (B) of the PAA gels on glass (■), aluminium (□) and pork skin (■), hardness of the gels (C) and cohesive strength of the gels (D).

To understand the biocompatibility of gels, BHK-21 cells were cultured (2D culture) in the presence of hydrogels prepared from **P1, P2** and **PAA** polymers. Interestingly, cell viability was increased within 24 hr in the presence of gels, as compared to control well with no added gel (Figure S19). **P2** showed the highest proliferation followed by **P1**, which

suggests the active role of adenine-dopamine adduct on the backbone of **P2**.

It has been reported that a mixture of polyacrylamide (PAAm) and Alg form hydrogel with increased stability and adhesive property than individuals.[26, 27] To evaluate the effect of mix polymer hydrogel on proliferation, Alg polymers incorporated with **3** (**P3)** and **6** (**P4)** were synthesized (Figure 1, SI Scheme 1C).[19, 20] They were successfully characterized using NMR & UV spectroscopic techniques where the new peaks in the aromatic region were originated because of functionalization on Alg polymer backbone (Figure 4A, Figure S20). **P3** showed 0.9±0.2 % and **P4** with 0.4±0.05 % degree of substitution by NMR.[17]

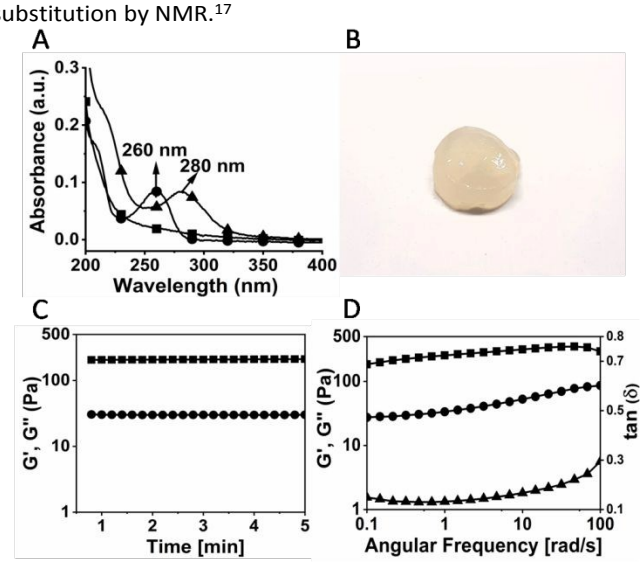

Figure4. UV-Vis spectra of polymers **P3** (—●—), **P4** (—▲—) and Alg (—■—) polymers (A), optical image of **P2P4** (1:1) gel (**B**), rheological properties -change in storage modulus G' (—■—) and in loss modulus G" (—●—) for **P2P4** hydrogel with respect to time (C) and frequency (D) along with loss factor for hydrogel tan (δ) (—▲—).

After successful characterization, the functionalized Alg polymers (**P3**&**P4**) were blended with functionalized PAA (**P1**&**P2**) and cross-linked to prepare **P1P3** and **P2P4** gels. Hydrogel prepared from adenine-dopamine adduct incorporated PAA and Alg polymers (**P2P4,** 1:1) was not transparent (Figure 4B) owing to the presence of Alg polymer and dopamine in the mixture.[28] Similarly, a 1:1 mixture of polymers **P1**&**P3** was also prepared to form gel in the same way and used for comparison. Rheological studies showed an increase in elastic modulus of **P2P4** gel (255 Pa) as compared to **P2** (188 Pa) at an applied frequency of 1 rad/s. The values of G' was consistently higher with respect to time, frequency and shear strain, as compared to the values of G" signifying its elastic nature (Figure 4C&D; Figure S21A). Moreover, the loss factor tan δ was below 0.5 for all frequencies tested indicating an excellent viscoelastic nature of the **P2P4** gel (Figure 4D).[23] Swelling ratio of the **P2P4** gel showed an increased rate of swelling for the first 24 hr and reached equilibrium near 72 hr in PBS (Figure S21B). Hydrogel formation was confirmed with the help of SEM analysis where the fully swollen freeze-dried hydrogel showed typical network gel morphology (Figure S21 C&D).

Cell Viability experiments showed an increase in cell density (BHK-21) within 24 hr, owing to increased proliferation on mixed **P2P4** (upto 7-8 folds) **& P1P3** gel than the control (without gel) and individual polymer components (Figure S22), suggesting a combined effect of Alg polymer derivatives and functionalized PAA. In order to understand the versatility of the gels, we also explored the proliferation of A431 human skin cancer cells. Normal 2D cell culture on a cover slip was employed as a control. The cell viability (2D culture) results showed an increase in cell density up to 3-4 folds for **P2P4** gel followed by **P2** gel within 24 hr (Figure 5A). The results are complemented with the observed increase in ATP production during the same time period (Figure 5B). The gels seeded with cells were incubated for 24 hr, removed from the culture media and cell morphologies & distribution were examined using confocal microscopy. The morphology of the cells did not change in the presence of **P2P4** or **P2** gel (Figure S23).

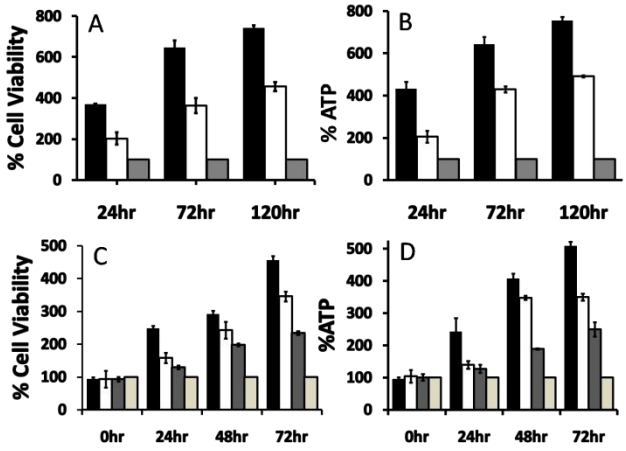

Figure 5. Cell viability (A) and ATP production (B) assays for A431 cells in presence of gels **P2P4** (■), **P2** (□) and control (■) in 2D cell culture. Cell viability (C) and ATP production (D) in presence of gels **P2P4** (■), P2 (□), PAA (■) and in the absence of gel (■) inside a 3D-culture of A431 skin cells.

The growth and penetration of cells inside the hydrogel was examined using z-stack imaging (Videos S2 and S3), indicating that cells grew inside the 3D- gel mimicking the biological environment. We also quantified the proliferation based on the analysis of intensity of nuclear staining using image J analysis[29]of the confocal micrographs. This showed an increase in intensity of nuclear stain with time, which further proves enhancement in proliferation of skin cells (Figure S24).

Hydrogels are excellent scaffolds for 3D-cell culture experiments because of their porous and viscoelastic characteristics which mimics the 3D-microenvironment of extracellular matrix (ECM).[30] We used a previously reported method for preparing 3D-cell culture of hydrogels.[31, 32] Here we premixed A431 cells with polymer solution and incubated for gelation at 37 °C for 6-7 hr (Figure S25). The *insitu* gelation was confirmed by upside-down tube method. Before incubation, it was free flowing viscous liquid but after incubation, the polymer solution was gelled nicely with no flow characteristics (Figure S26). Cell density was measured at different time points and **P2P4** gel showed maximum

proliferation followed by **P2** and then **PAA** (Figure 5C). Normal control was also set up without hydrogel for comparison. Cell viability was increased to more than 2 times than the control (without gel) in 24 hr for the **P2P4** gel, which continues inside the gel up to 72 hr, where the cell density was increased to nearly 5 times (Figure 5C&D). The increased concentration of ATP observed reflects the cell density and confirms the enhancement in proliferation of cells (Figure 5D). The cell morphology of the **P2P4** and **P2** gels did not change and remain intact for 3 days, while cell density increased significantly indicating the proliferation of healthy cells (Figure 6). The z-stack image confirmed that the cells are grown inside the 3D - gel (Video S4 and S5). The enhanced proliferation was further confirmed by analysis of nuclear stain by image J software (Figure S27).[29]

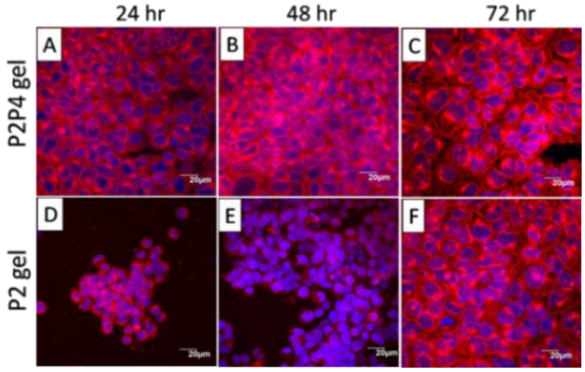

Figure 6. Confocal microscopic images of cells seeded in 3D hydrogels (**P2P4**&**P2**), at different time points, (A&D – 24 hr; B&E – 48 hr and C&F – 72 hr).

In conclusion, we designed and synthesized adenine and adenine-dopamine adduct immobilized PAA (**P1**, **P2**) and Alg polymers (**P3**, **P4**). **P2** showed excellent adhesion to various substrates, including pork skin as compared to **P1** and **PAA**. The **P2** gel showed a 5 folds enhancement in the proliferation of BHK-21 and human skin cancer cell line, A431 in 2D cell culture followed by **P1** gel within 24 hr. The blended **P2P4** (1:1) gel showed enhanced strength modulus and high cell proliferation activity as compared to **P2** gel. In 2D and 3D cell culture models, **P2P4** gel showed 2-4 fold enhancement in the proliferation of A431 cells in 24 hr followed by **P2**. These nucleobase functionalized polymer gels also showed strong adhesive properties, increased hardness, transparency, biocompatibility, and induced cell proliferation in both 2D- and 3D-cell culture models. Such materials could be further explored for developing functional scaffolds for regenerative medicines, wound healing and tissue engineering.

We gratefully thank Madam Jiang Xiaohui, Ms. Huang Min and Prof Yang Hongshun at the Food Science and Technology centre, NUS for their guidance regarding texture analysis and rheological measurements. We gratefully acknowledge funding support from the National University of Singapore (A-143-000-A76-113) and PhD scholarship through IITK-NUS joint degree program. Sandeep Verma thanks SERB for JC Bose Fellowship.

Conflicts of interest

"There are no conflicts to declare".

View Article Online
DOI: 10.1039/D0CC04909C

Notes and references

1 A. C. Daly, L. Riley, T. Segura and J. A. Burdick, *Nat. Rev. Mater.*, 2020, **5**, 20-43.
2 C. A. Cezar, E. T. Roche, H. H. Vandenburgh, G. N. Duda, C. J. Walsh and D. J. Mooney, *Proc. Natl. Acad. Sci.*, 2016, **113**, 1534-1539.
3 C. Ghobril and M. W. Grinstaff, *Chem. Soc. Rev.*, 2015, **44**, 1820-1835.
4 S. Tamesue, T. Endo, Y. Ueno and F. Tsurumaki, *Macromolecules*, 2019, **52**, 5690-5697.
5 S. Liang, Y. Zhang, H. Wang, Z. Xu, J. Chen, R. Bao, B. Tan, Y. Cui, G. Fan, W. Wang, W. Wang and W. Liu, *Adv. Mater.*, 2018, **30**, 1704235.
6 M. W. Tibbitt and K. S. Anseth, *Biotechnol. Bioeng.*, 2009, **103**, 655-663.
7 T. Billiet, M. Vandenhaute, J. Schelfhout, S. Van Vlierberghe and P. Dubruel, *Biomaterials*, 2012, **33**, 6020-6041.
8 M. C. Cushing and K. S. Anseth, *Science*, 2007, **316**, 1133-1134.
9 A. Hickman, R. Graeser, R. de Hoogt, S. Vidic, C. Brito, M. Gutekunst and H. van der Kuip, *Biotechnol. J.*, 2014, **9**, 1115-1128.
10 S. Van Vlierberghe, P. Dubruel and E. Schacht, *Biomacromolecules*, 2011, **12**, 1387-1408.
11 P. S. Yavvari, S. Pal, S. Kumar, A. Kar, A. K. Awasthi, A. Naaz, A. Srivastava and A. Bajaj, *ACS Biomater. Sci. Eng.*, 2017, **3**, 3404-3413.
12 S. Verma, A. K. Mishra and J. Kumar, *Acc. Chem. Res.*, 2010, **43**, 79-91.
13 D. Wang, C. Yu, L. Xu, L. Shi, G. Tong, J. Wu, H. Liu, D. Yan and X. Zhu, *J. Am. Chem. Soc.*, 2018, **140**, 8797-8806.
14 J. Saiz-Poseu, J. Mancebo-Aracil, F. Nador, F. Busqué and D. Ruiz-Molina, *Angew. Chem. Int. Ed.*, 2019, **58**, 696-714.
15 G. M. Peters and J. T. Davis, *Chem. Soc. Rev.*, 2016, **45**, 3188-3206.
16 M.-J. Yin, M. Yao, S. Gao, A. P. Zhang, H.-Y. Tam and P.-K. A. Wai, *Adv. Mater.*, 2016, **28**, 1394-1399.
17 Y. Matsumoto, D. Ishii and T. Iwata, *Carbohydr. Polym.*, 2017, **171**, 229-235.
18 T. Chen, Y. Chen, H. U. Rehman, Z. Chen, Z. Yang, M. Wang, H. Li and H. Liu, *ACS Appl. Mater. Interfaces*, 2018, **10**, 33523-33531.
19 J. Shin, J. S. Lee, C. Lee, H.-J. Park, K. Yang, Y. Jin, J. H. Ryu, K. S. Hong, S.-H. Moon, H.-M. Chung, H. S. Yang, S. H. Um, J.-W. Oh, D.-I. Kim, H. Lee and S.-W. Cho, *Adv. Funct. Mater.*, 2015, **25**, 3814-3824.
20 K. D. Addisu, B. Z. Hailemeskel, S. L. Mekuria, A. T. Andrgie, Y.-C. Lin and H.-C. Tsai, *ACS Appl. Mater. Interfaces*, 2018, **10**, 5147-5160.
21 L. Zhao, J. Huang, Y. Zhang, T. Wang, W. Sun and Z. Tong, *ACS Appl. Mater. Interfaces*, 2017, **9**, 11866-11873.
22 K. M. Mabry, R. L. Lawrence and K. S. Anseth, *Biomaterials*, 2015, **49**, 47-56.
23 X. Liu, Q. Zhang, L. Duan and G. Gao, *Adv. Funct. Mater.*, 2019, **29**, 1900450.
24 X. Liu, Q. Zhang, K. Li, L. Duan and G. Gao, *Chem. - Eur. J.*, 2018, **24**, 15119-15125.
25 J. Hurler, A. Engesland, B. Poorahmary Kermany and N. Škalko-Basnet, *J. Appl. Polym. Sci.*, 2012, **125**, 180-188.
26 J. Li, A. D. Celiz, J. Yang, Q. Yang, I. Wamala, W. Whyte, B. R. Seo, N. V. Vasilyev, J. J. Vlassak, Z. Suo and D. J. Mooney, *Science*, 2017, **357**, 378-381.
27 J.-Y. Sun, X. Zhao, W. R. K. Illeperuma, O. Chaudhuri, K. H. Oh, D. J. Mooney, J. J. Vlassak and Z. Suo, *Nature*, 2012, **489**, 133-136.
28 A. Cholewinski, F. K. Yang and B. Zhao, *Langmuir*, 2017, **33**, 8353-8361.
29 S. Fontenete, D. Carvalho, A. Lourenço, N. Guimarães, P. Madureira, C. Figueiredo and N. F. Azevedo, *Biochem. Eng. J.*, 2016, **112**, 61-69.
30 H. Zhan and D. W. P. M. Löwik, *Adv. Funct. Mater.*, 2019, **29**, 1808505.
31 J. S. Temenoff, H. Shin, D. E. Conway, P. S. Engel and A. G. Mikos, *Biomacromolecules*, 2003, **4**, 1605-1613.
32 T. S. Wilems, X. Lu, Y. E. Kurosu, Z. Khan, H. J. Lim and L. A. Smith Callahan, *J. Biomed. Mater. Res. A*, 2017, **105**, 3059-3068.

View Article Online
DOI: 10.1039/D0CC04909C

View Article Online
DOI: 10.1039/D0CC04909C

TOC graphic

Bioinspired Adenine-Dopamine Immobilized Polymer Hydrogel Adhesive for Tissue Engineering

Saurabh Joshi, Gomathi Mahadevan, Sandeep Verma, Suresh Valiyaveettil**

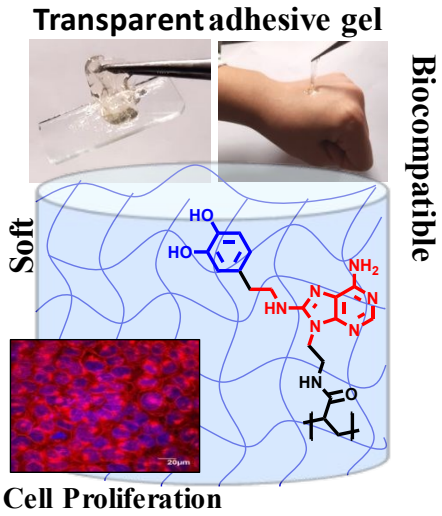

Adenine – dopamine adduct incorporated polyacrylic acid forms hydrogels with enhanced adhesiveness, transparency, biocompatibility and promote cell proliferation in in vitro models within 24 hr.